Engineering Structures 301 (2024) 117189

Contents lists available at ScienceDirect

Engineering Structures

journal homepage: www.elsevier.com/locate/engstruct

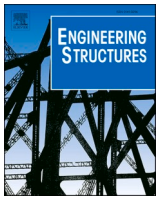

Quantifying the effect of end support restraints on vibration serviceability of mass timber floor systems: Testing

Sigong Zhang [a,*], Ying Hei Chui [b]

[a] School of Engineering, Newcastle University, Newcastle upon Tyne NE1 7RU, UK
[b] Department of Civil and Environmental Engineering, University of Alberta, Edmonton, AB T6G 1H9, Canada

ARTICLE INFO

Keywords:
Mass timber floor systems
Vibration serviceability
Cross-laminated timber
End support restraints
End fixity factor

ABSTRACT

Design of mass timber floor systems is commonly governed by vibration serviceability due to high stiffness-to-weight ratio and low inherent damping of timber. Research and design practice have shown that static deflection under a concentrated load and fundamental natural frequency can be effective and robust indicators for vibration performance of mass timber floors. These design parameters are normally calculated by assuming simply supported conditions in existing design methods. However, such an assumption deviates from actual floor supports, especially in platform-framed buildings, and in-situ end support restraints have been widely recognized as a significant factor affecting the vibration performance. The purpose of the study is to quantify the influence of end support restraints on vibration serviceability of mass timber floors in platform construction through a comprehensive experimental program and analytical treatment. This paper is the first part and focus specifically on the experimental work on cross-laminated timber (CLT) panels. In particular, extensive laboratory tests have been conducted on different CLT floor panels with various end support restraints induced by top loads, self-tapping screws and steel angle brackets. The fundamental natural frequency and mid-span deflection under a concentrated load were measured for each end support configuration. The rotational restraint stiffness was determined by comparing results of restrained supports to those of simple supports and represented as end fixity factors. The analysis of test results shows that the CLT floor-to-wall connection exhibited inherent non-linear behaviour and such characteristic was more significant for higher top loads. Compared with screws and brackets, the top loads dominated the partially restrained effect but such dominance gradually diminished for lower-level top loads. In addition, support wall thickness notably impacts the support restraint. It was then suggested that the clear span could be used to determine deflection and frequency in the design, but further investigation is needed.

1. Introduction

In recent decades, mass timber panels (MTP) have emerged as a practical and promising solution for mid-rise wood construction, particularly as floor and wall elements [1]. One of the most well-known MTP products is cross laminated timber (CLT), but other unidirectional options such as glued laminated timber (GLT), dowel-laminated timber (DLT) and nailed laminated timber (NLT) are beginning to attract the attention of designers as viable products for floor construction. The growing interest in and demand for MTP constructions has brought forth numerous design challenges, especially regarding vibration performance induced by human activities, as mass timber floors are lighter in weight and have lower inherent damping than conventional concrete or steel-concrete composite floors. Therefore, vibration performance is a critical serviceability concern for these systems and is more likely to govern the design [2,3].

Vibration serviceability of timber floors due to human activities is a complex issue involving multiple factors. Over the last few decades, significant efforts have been made to reduce the level of complexity by identifying important performance indicators, developing statistics-based performance criteria, and creating analytical models for design parameters. This has paved the way for development of design approaches. One commonly used method for timber floors is to employ the static deflection under a concentrated load (usually 1 kN) and the fundamental natural frequency as design parameters [4–8]. This method has also been applied to the vibration design of mass timber floors [2,9,

* Corresponding author.
E-mail address: sigong.zhang@newcastle.ac.uk (S. Zhang).

https://doi.org/10.1016/j.engstruct.2023.117189
Received 11 July 2023; Received in revised form 27 October 2023; Accepted 18 November 2023
Available online 9 December 2023

10].

However, current design methods generally assume simple support conditions for calculating natural frequency and deflection, which deviates from actual floor boundary conditions in mass timber floors, especially in platform-framed buildings. In reality, these floors are commonly sandwiched between walls of adjacent storeys and mechanically fastened with wall panels. As a result, the upper surface of floor slabs over the support is restrained by upper-storey loads, referred to as top loads herein, leading to a clamping action or a partially restrained effect at end supports [11]. Moreover, various floor-to-wall fasteners, such as self-tapping screws (STS), steel brackets, and metal plates can also introduce additional restraints. In a general overview of CLT development, Brandner et al. [12] have proposed the need to quantify the impact of end support restraints caused by semi-rigid connections, as well as the influence of the upper-storey loads transmitted through wall panels on floor performance.

In recent years, a number of studies have been conducted to investigate the influence of end support conditions on the performance of mass timber floors. Among the earliest test studies, Weckendorf and Smith [13] employed mechanical clamps to secure the edges of CLT floor slabs to the top flange of steel I-beam supports. Their findings revealed an approximate 5% increase in fundamental natural frequencies and a 10% reduction in damping for CLT floors that were clamped compared to those simply resting on the I-beam supports. In parallel, Hernandez and Chui [14] investigated the effect of fastening all four edges of CLT slabs with STS, reporting an average increase of 5% for fundamental natural frequencies of fastened floors compared to those with four edges simply-supported. Subsequently, Hernandez and Chui [15] carried out further laboratory tests to examine the vibrational behaviour of a 3-ply CLT panel supported on two end supports with different conditions, including superimposed top loads and STS connections. They varied the top loading levels between 5 kN/m and 30 kN/m and increased the number of STSs from 1 to 13 on each end support. Measurements were taken for both the mid-span deflection under a 1 kN concentrated load and the fundamental natural frequency were measured. They observed that as the top loads and the number of screws increased, the fundamental natural frequency increased and the static deflection decreased. Meanwhile, damping ratios remained fairly constant at approximately 1%. Additionally, tests were conducted to assess the rotational stiffness of various support conditions in an isolated connection test setup.

More recently, Zimmer and Augustin [16] conducted both laboratory tests and in-situ measurements to study the effect of top loads, support elastomers and dead loads on vibration behaviour of CLT floors. They found that the influence of elastomers can be neglected, but the clamping effect at the supports due to the load of superimposed storeys should be taken into account in calculation. Other factors such as the span and the width of the supports also have a major role on the degree of clamping. Apart from the previously mentioned one-way CLT slab tests (i.e., supported on two sides), a two-way laboratory-scale CLT floor system was tested by Chúláin and Harte [17] to investigate the influence of STSs, steel brackets and added mass on vibration behaviour of CLT floors. Their study indicated that the STS spacing had negligible influence on the fundamental frequency, but the addition of steel brackets increased the fundamental frequency by up to 6%, with an 11% reduction in the static point load deflection. Moreover, they also found that the added mass resulted in a reduction of the fundamental frequency by more than 25%.

In addition to conducting physical tests, many efforts were dedicated to numerical modelling. Using 3D shell elements with linear elastic orthotropic material properties, finite element modelling was performed in [18] to analyse the influence of different support conditions on serviceability deflection and natural frequencies for both one- and two-way CLT floor systems. They examined a range of support conditions, including fully fixed, semi-rigid (i.e., partially restrained) and simply-supported. The study indicated that the mid-span deflection and vibration response are significantly influenced by end support restraints and the number of edges supported. Notably, increasing the degree of support fixity could reduce mid-span deflection by up to 79%, while the fundamental frequency increased by 23% and 99% for semi-rigid and fully clamped support conditions, respectively. Similarly, Ussher et al. [19] carried out numerical modelling to study effects of boundary support conditions, focusing specifically on comparison between free and simply supported cases (e.g., four edges simply supported and two opposite edges simply supported and the other two free).

Although the aforementioned testing and modelling studies shed some lights on the vibrational behaviour of mass timber floors with restrained supports and highlighted the need to further quantify the influence of various end support conditions, few practical approaches are available to consider the effect of partially restrained supports in design. A frequency factor was introduced in [20] to account for the impact of restrained support conditions in frequency calculations. This factor considers only four types of boundary conditions, namely cantilever, simply supported, one end simply supported and the other end fully clamped, and both ends fully clamped. These conditions are idealized extreme conditions that do not reflect actual end support conditions in mass timber floors either. In reality, it is highly challenging, if not impossible, to achieve fully clamped conditions that restrain all displacement components at supports, especially for wood.

A more realistic end support exhibits semi-rigid deformation behaviour. That is, for instance, a simply-supported connection possesses a certain amount of rotational stiffness, while a fully clamped joint contains some degree of rotational fixity flexibility. To address this issue, Malo and Köhler [21] implemented a beam with a rotational spring at each end to represent mass timber floors with restrained boundary conditions. They derived simple formulas to calculate the fundamental natural frequency and mid-span deflection under a concentrated load. Most recently, the restrained beam model was also adopted by Zhang et al. [11] to investigate the effect of end support restraints in CLT floors. Instead of using the rotational stiffness, they employed an end fixity factor to quantify end support restraints, which is normalised with floor flexural stiffness and span. The end restraint coefficients were then expressed as a function of the end fixity factor, which can be applied to corresponding simply-supported beam equations to calculate the deflection and fundamental natural frequency, accounting for the effects of end support restraints. The analytical approach was validated using test results reported in Hernandez and Chui [15].

The above-mentioned research activities have contributed to the understanding of the impact of end support restraints on vibration behaviours of mass timber floors. However, further testing and analytical modelling are necessary to move beyond qualitative conceptualizations and quantify the influence of a broader range of floor-to-wall connections. This study aims to fill this research gap. The purpose was two-fold: first, to characterize the end support restraints, not only for serviceability design but also for bending strength in the future; and second, to identify the governing factors for practical designs.

In this study, comprehensive experimental work was conducted on CLT floor slabs with various end support conditions, including top loads, STS, steel angle brackets (SAB), and their combinations. Four CLT slabs with different thicknesses were included, and at least three spans were made from each slab. Other variables, such as top loading levels, screw number and length, provision of steel brackets and wall support width, were thoroughly examined. Based on the test results, the initial focus was on investigating the nonlinear behaviour of floor-to-wall connections, followed by the determination of end fixity factors for deflection and frequency calculations. The governing factors were then established by comparing different combinations of floor-to-wall connections, and the impact of wall support thickness was also assessed.

2. Mass timber floor-to-wall connections and theoretical models

2.1. Typical floor-to-wall connections in platform-framed buildings

Mass timber buildings, particularly those made with CLT, are typically erected using platform or balloon-framed techniques that connect wall panels and floor slabs with STSs in combination with SABs, as illustrated in Fig. 1. In platform construction, mass timber floor slabs are commonly installed between the vertical wall panels, with the lower walls supporting the floor slab and the upper walls placed on top of the slab.

There are many different types of fastening systems that can be used to join CLT floor slabs and wall panels. The most straightforward approach to connecting a CLT floor to wall panels is to use long, partially-threaded STSs, which are driven directly into the narrow side of the wall edge, as demonstrated in Fig. 2 [2]. Commonly used STSs are available in many combinations of diameters, lengths, head and thread types, with the screw installation angles, spacings and end/edge distances specified by manufacturers. The screw diameter is normally 8 mm, and the screw length ranges from 160 mm to 400 mm, depending on the floor slab thickness. SABs are also commonly used to connect floors to walls both above and below, using screws and nails. These brackets are made from galvanised or stainless steel with a thickness of 1.5–3 mm and a hole diameter of 5 mm for anchor nails or screws. Typically, these brackets are installed with a spacing of 300–500 mm. Both STS and SAB have many sub-types designed specifically for different applications. In addition, many innovative fastening techniques and systems, such as concealed metal plates, have been effectively utilised to connect mass timber floor slabs to wall panels [2].

2.2. End restraint coefficients and end fixity factors

Rotational restraints occur at floor-to-wall connections in multi-storey mass timber buildings due to hindered rotations of floor slabs, as shown in Fig. 3. These restraints at end supports can decrease deflections and increase natural frequencies compared to those of a simple support system. To quantify the effect of end support restraints on the vibration serviceability of mass timber floor systems, dimensionless coefficients were introduced in [11] for the mid-span deflection under a concentrated load and the fundamental frequency of rotationally-restrained beams. It follows that, for a restrained beam, the mid-span deflection under a 1 kN concentrated load, d_{1kN}, and the fundamental natural frequency, f_1, can be calculated as follows:

$$d_{1kN} = C_d \frac{PL^3}{48EI} \tag{1}$$

$$f_1 = C_f \frac{\pi}{2L^2}\sqrt{\frac{EI}{\rho A}} \tag{2}$$

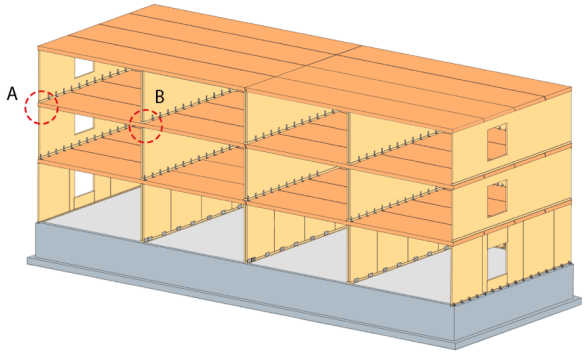

Fig. 1. Typical floor supports in a platform-framed mass timber building (red dotted circles: **A** – end support, and **B** – mid-support).

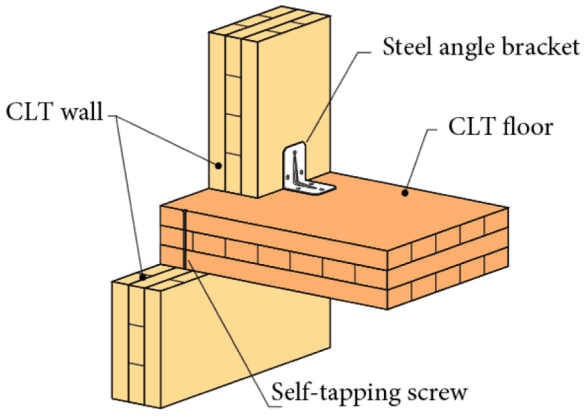

Fig. 2. Typical CLT floor-to-wall connections in platform-framed construction (end support as A in Fig. 1).

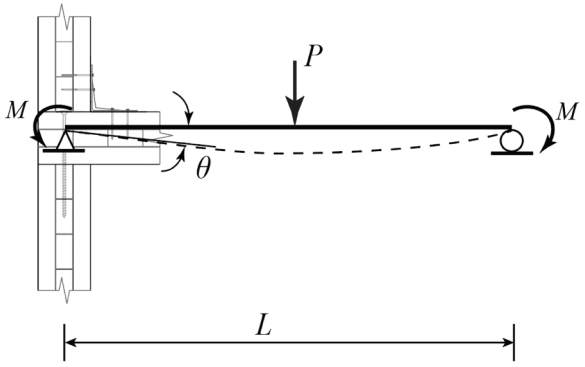

Fig. 3. Schematic diagram of mass timber floors with end support restraints.

in which P is the concentrated load; L is the floor span; EI is the flexural stiffness; ρ is the density; A is the section area; and C_d and C_f were denoted as end restraint coefficients in [11], which can be incorporated into the current design formulas intended for simple support conditions (e.g., CSA O86–19 [10]). These coefficients are dependent on the rotational stiffness $R = M/\theta$ as shown in Fig. 3, and analytical expressions can be derived to express C_d and C_f in terms of the rotational stiffness as reported in Malo and Köhler [21].

In lieu of the rotational stiffness, a end fixity factor was proposed to characterise end support restraints [11], which is defined as

$$r = \frac{1}{1 + 3\frac{EI}{RL}} \tag{3}$$

where R is the rotational stiffness of end support restraints, EI is the flexural stiffness of the CLT panels, and L is the span. The end fixity factor varies from 0 to 1, with values of 0 and 1 representing simply-supported and fully clamped conditions, respectively. This allows engineers to characterise the end fixity in an intuitive manner. By implementing the end fixity factors, the end restraint coefficients C_d and C_f were derived in [11] as follows:

$$C_d = \frac{5r^2 - 18r + 16}{16 - 4r^2} \tag{4}$$

$$C_f = 3.94\sqrt{\frac{8 - 2r - 3r^2}{124 - 182r + 67r^2}} \tag{5}$$

It should be noted that the shear flexibility of CLT panels was not considered in the derivation of Eqs. (4) and (5). Based on the measured mid-span deflection and fundamental natural frequency, end restraint coefficients can be obtained by comparing deflection and frequency

measurements of restrained beams with those of simply supported beams. Once the end restraint coefficient is determined, the end fixity factor for each end support configuration can be calculated using Eqs. (4) or (5). In this manner, using Eq. (4), the end fixity factor for deflection, r_d, can be expressed as

$$r_d = \frac{9 - \sqrt{81 - (5 + 4C_d)(16 - 16C_d)}}{5 + 4C_d} \tag{6}$$

Similarly, the end fixity factor for frequency, r_f, can be given by

$$r_f = \frac{5.86C_f^2 - 1 - \sqrt{25 - 1.16C_f^2 - 0.11C_f^4}}{4.32C_f^2 + 3} \tag{7}$$

By following this procedure, the end fixity factor for a specific floor-to-wall connection can be determined through experimental investigations. However, to develop an empirical formula that covers a wide range of floor-to-wall connections, a comprehensive experimental study is necessary, as will be described below.

3. Experimental work

While a variety of MTPs can be employed in mass timber floors, this test program focuses on CLT slabs. Similar tests can be conducted for other MTP products, and the results can be used to validate design formulas developed based on CLT tests.

3.1. Test setup

The test setup used in this study was adapted from Zimmer and Augustin [16] and is depicted in Fig. 4 and Fig. 5. The CLT floor slab was supported by 300 mm tall × 800 mm long CLT wall segments. The upper CLT wall segments, which was 150 mm tall, were mounted on the floor panel and fixed by using steel hollow structural sections (100 mm × 100 mm × 6 mm) and two threaded rods (Ø 19 mm) loaded by hollow hydraulic cylinders (Enerpac® RCH-123). These steel rods were anchored to the concrete strong floor using anchor holes placed at 0.6 m (2 ft) intervals in both horizontal and vertical directions.

The hydraulic cylinders located at end supports were implemented to simulate top loads transmitted from upper storeys through walls. The load in one cylinder was manually controlled using a hand pump with a pressure gauge installed, and the hydraulic pressure was monitored by gauges with a range up to 13.8 MPa (2000 psi). By calibrating the hydraulic pressure to load, the clamping force can be monitored. The two actuators can apply a maximum load of 49 kN.

For static deflection tests, a concentrated load was applied at mid-span using either steel blocks, as shown in Fig. 5a (each block weighing 22.7 kg), or hydraulic cylinders (Fig. 5b). When using steel blocks, three load levels were applied, namely 0.9 kN, 1.8 kN and 2.7 kN, and some tests used an applied load up to 3.6 kN. If hydraulic cylinders were employed to apply the load at mid-span, six load levels were imposed: 2.8 kN, 5.2 kN, 7.7 kN, 10.2 kN, 12.6 kN and 15.1 kN. For each applied load, deflection was measured below the CLT floor panel at mid-span with two cable transducers installed on both sides.

The fundamental natural frequency was also measured for all CLT panels with different end support restraints in addition to the static deflection tests. The CLT panel was excited into free vibration by striking it with an instrumented hammer, and the vibration response was measured by an accelerometer attached to the CLT panel. The impact and response acceleration time history signals were recorded and analysed by modal analysis software (RT Pro 6.33, Brüel & Kjær) to produce frequency response function, from which the fundamental natural frequency was determined. Each frequency measurement was repeated three times.

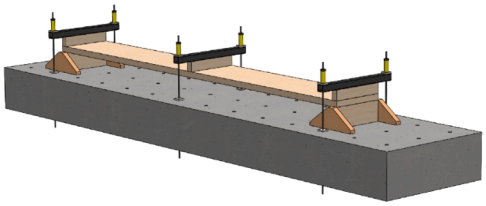

Fig. 4. Schematic diagram of the test setup.

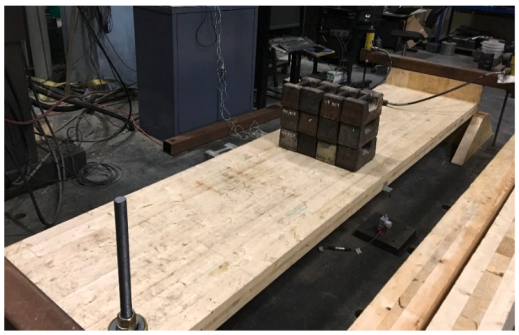

(a) Steel blocks at mid-span

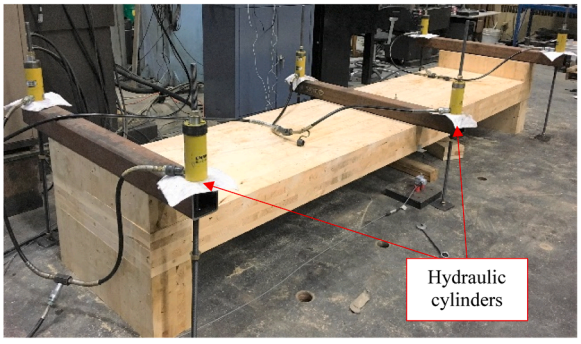

(b) Hydraulic cylinders at mid-span

Fig. 5. The test setup for static load applications.

3.2. Materials

The CLT panels used in this study was E1 grade panels according to ANSI/APA PRG 320 standard [22]. The longitudinal laminates are 1950 F_b-1.7E spruce-pine-fir (SPF) machine stress rated lumber and No. 3/Stud grade SPF lumber was used in the transverse layers. The average moisture content was in the range of 8.5–11%, which was measured using an electrical resistance moisture meter. The average measured density was 515 kg/m^3. In total, four CLT panels with width of 0.8 m were tested, with thicknesses of 89 mm, 105 mm, 175 mm, and 244 mm, respectively. Among them, the 89 mm and 105 mm CLT panels consisted of three layers of lumber, while the 175 mm and 244 mm panels have five and seven layers, respectively. These CLT panels are denoted by 89–3s, 105–3s, 175–5s and 244–7s

Four different spans of CLT panels were tested, namely 6.1 m (20 ft), 4.9 m (16 ft), 3.6 m (12 ft), and 2.4 m (8 ft). These span lengths were measured between centrelines of end supports. The actual length of a CLT panel is the span plus support width (i.e., wall thickness). For each panel, the longest span was first tested, and the length was progressively reduced to allow the other shorter span specimens to be tested.

To fasten floor slabs to wall supports, partial thread STSs with the same diameter but different lengths were used. The diameter of the screws was 8 mm, and the length ranged from 160 mm to 340 mm, depending on the thickness of the CLT slabs. Table 1 shows the dimensions of the screws used in the four CLT panels. The SABs, as shown in Fig. 6, were fastened to the wall and floor panels using eight Ø

Table 1
Self-tapping screws used in CLT floor-to-wall connections.

Model	Diameter (mm)	Total Length (mm)	Thread length (mm)	CLT panel
PTS8160	8	160	80	89–3s
PTS8240	8	240	80	105–3s
PTS8280	8	280	80	175–5s
PTS8340	8	340	100	244–7s

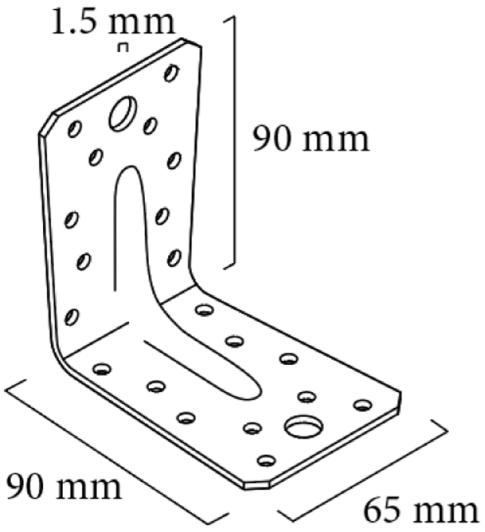

Fig. 6. Size of steel angle brackets.

5 × 40 mm round-head screws (four screws on each leg of a bracket).

3.3. Test matrix

A total of fifteen CLT floor-to-wall assemblies were tested, consisted of four CLT panels of different thicknesses and four span lengths (The 244–7s panel with a 2.4 m span was not tested). For each assembly, more than ten end-support configurations were examined, including top loads, STSs, or SABs. Both end supports of each assembly had the same arrangement. Table 2 summarises all assemblies and their end support configurations. The order of end support configurations in Table 2 reflects the actual test sequence, starting with the simply supported condition, followed by gradually applying top loads on end supports from 6 kN/m to 60 kN/m. The applied load levels were determined based on the weight of bare CLT storeys. For instance, a 6 kN/m load is equivalent to the dead load applied due to a one-storey of 5 m span floor and 3 m high walls built with 3-layer CLT panels. After the top load tests, SABs and STSs were installed. The spacing between connectors was 300 mm for three brackets (3SAB) or screws (3STS) and 150 mm for five brackets (5SAB) and screws (5STS). Only upper wall segments were connected to the floor panels using brackets as shown in Fig. 7. In total, five types of end support configurations were created, namely load, load+SAB, STS, Load+STS and Load+STS+SAB.

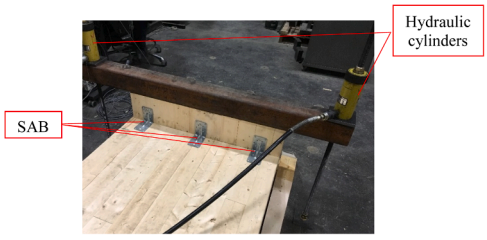

Fig. 7. Installation of three steel angle brackets (only installed on upper wall segment).

Table 2
Test program of CLT floor-to-wall assemblies.

End-support configurations		CLT floor-to-wall assemblies						
		89–3s			105–3s	175–5s		244–7s
		Span (m)						
		6.1	4.9	3.6 2.4	6.1 4.9 3.6 2.4	6.1 4.9	3.6 2.4	6.1 4.9 3.6
Simple supports	SS (0)	✓	✓	✓	✓	✓	✓	✓
Top load (kN/m)	6	✓	✓	✓	✓	✓	✓	✓
	12	✓	✓	✓	✓	✓	✓	✓
	24	✓	✓	✓	✓	✓	✓	✓
	36	✓	✓	✓	✓	✓	✓	✓
	48	✓	✓	✓	✓	✓	✓	✓
	54	×	×	×	×	×	×	✓
	60	✓	✓	✓	✓	✓	✓	×
Top load + SAB	60 + 3SAB	✓	✓	✓	✓	✓	×	×
	36 + 3SAB	✓	✓	✓	✓	✓	×	×
	12 + 3SAB	✓	✓	✓	✓	✓	×	×
	12 + 5SAB	✓	×	✓	×	×	×	×
	36 + 5SAB	✓	×	✓	×	×	×	×
	60 + 5SAB	✓	×	✓	×	×	×	×
STS	3STS	✓	✓	✓	✓	✓	✓	✓
	5STS	✓	✓	✓	✓	✓	✓	✓
Top load + STS	12 + 5STS	✓	✓	✓	✓	✓	✓	✓
	36 + 5STS	✓	✓	✓	✓	✓	✓	✓
	54 + 5STS	×	×	×	×	×	✓	✓
	60 + 5STS	✓	✓	✓	✓	✓	×	×
Top load + STS + SAB	60 + 5STS+ 5SAB	✓	×	×	×	×	×	×

Note: STS = self-tapping screws; SAB = steel angle brackets

For ease of identification of each assembly type, the following designation was adopted:

CLT thickness – (support thickness) - span - loading + STS and its number + SAB and its number

For instance, specimen **CLT89-(S89)− 6.1–60 + 5STS+ 5SAB** denotes a panel that is 89 mm thick, has a span of 6.1 m span, and is subject to a load of 60 kN/m. The designation also indicates that the panel is supported at both ends with 89 mm thick supports, and has been affixed with 5 STS and 5 SAB. While the width of the support (e.g., **S89**) may or may not be included in the designation, other details such as the length of the screws may be specified separately.

Table 3 outlines the end support variables investigated in the present test program, which was designed to focus more on the parameters that are considered more influential. The support configurations that involve top loads and STSs were thoroughly investigated for all assemblies as they are considered more critical than SABs. On the other hand, SAB conditions were mainly adopted for 89–3s CLT panels, as they play a minor role, to reduce the total number of test configurations. Additionally, other factors such as screw length and wall support thickness were also studied. For CLT89 and CLT105 assemblies, wall supports were manufactured using 89–3s panels (i.e., S89), while 105–3s and 175–5s CLT panels were used for wall supports of CLT175 and CLT244 assemblies, denoted as S105 and S175. More detailed test arrangements for these factors will be elaborated in subsequent sections of test results and discussions.

4. Test results

The mid-span deflections under multi-level concentrated loads and fundamental frequency were measured for each end support configuration, and the data can be found in supplemental files. By comparing the data of configurations with end support restraints to those of simple support conditions, the end restraint coefficients, C_d and C_f, can be obtained using Eqs. (1) and (2), followed by inversely determining the associated end fixity factors based on Eqs. (6) and (7). It should be noted that end support restraints should be considered for both strength and serviceability in the design of timber floors. Therefore, prior to examining the end fixity factor used for vibration serviceability, the nonlinear characteristic of CLT floor-to-wall connections was analyzed first.

4.1. Nonlinear behaviour and stiffness degradation

CLT floor-to-wall connections can be essentially classified as semi-rigid, which could exhibit non-linear force-rotation behaviour over a range of loading, similar to most types of beam-to-column connections in steel frames [23]. Although floor vibration serviceability can always fall into the linear elastic category by using the initial stiffness to represent the connection behaviour, it is necessary to interpret the non-linear feature of floor-to-wall connections and specify the relevant loading on floors to determine the rotational stiffness and end fixity factor. However, previous experimental studies [15–17] only measured deflection due to a 1 kN load applied at midspan, providing no information on the nonlinearity of CLT floor-to-wall connections. Hence, multi-level mid-span loadings had been applied during the tests for the first time to exemplify the non-linear nature of tested floor-to-wall connections.

The mid-span deflections were measured for multi-level concentrated loads for each end support configuration, and the load-deflection curves for CLT89–6.1 assembly with various top loads are shown in Fig. 8a. Upon initial observation, linear behaviour was evident for each configuration. However, upon closer examination, it was found that slope slightly changes with the increase of concentrated load. Fig. 8b illustrates slope changes for each load-deflection curve. It suggests that no slope change can be found for the simple support condition (CLT89–6.1-SS), but slopes decrease with higher applied concentrated loads for loaded support conditions (CLT89–6.1–6 to 60). In particular, such a slope decrease is more significant for larger top loads. This implies that the restrained effect by the top load over the support tends to be diminished with the increase of external loading on the panels. Such a phenomenon can be further explained by using end fixity factors. Fig. 9 presents end fixity factor values obtained by using deflection ratios under different mid-span concentrated loads. It can be observed that the fixity factor gradually decreases with the increase of concentrated loads, and the rate of decrease was accelerated for larger end support top loads. Such stiffness reduction can be referred to as rotational stiffness degradation.

Similar degradation of rotational stiffness can also be found for other end support configurations with screws or brackets. To consider the degradation of rotational stiffness, it is necessary to determine the end fixity factor based on the level of loading on floors. Currently, the design parameter for vibration serviceability of mass timber floors commonly use floor deflection subjected to 1 kN concentrated load at mid-span [9]. Hence, in this study, the end fixity factors for deflection were determined using1 kN concentrated load at mid-span. The mid-span deflection under 1 kN concentrated load, d_{1kN}, was obtained by using linear interpolation on the load-deflection curves and presented in the supplemental files.

4.2. End fixity factors for deflection and frequency

The methodology used to determine the end fixity factor in Section 2.2 is a simple approach for identifying boundary conditions, which has been extensively investigated for aircraft (e.g., [24]) and highway bridges (e.g., [25]). The boundary stiffness can be identified using modal parameters such as natural frequencies or static response (e.g., static

Table 3
End support variables for different floor-to-wall assemblies.

CLT	Span (m)	Support	End support variables						
			Load	No. of STS	STS length	Load + STS	Load + SAB	Load + STS + SAB	Support thickness
CLT89	6.1	S89	✓	✓	×	✓	✓	✓	×
	4.9/3.6/2.4	S89	✓	✓	×	✓	✓	×	×
CLT105	6.1	S89	✓	✓	✓	✓	✓	×	×
	4.9/3.6/2.4	S89	✓	✓	×	✓	✓	×	×
CLT175	6.1	S105	✓	✓	×	✓	✓	×	×
	4.9	S105 or S175	✓	✓	×	✓	✓	×	✓
	3.6	S105 or S175	✓	✓	×	✓	×	×	✓
	2.4	S105	✓	✓	×	✓	×	×	×
CLT244	6.1/4.9/3.6	S105 or S175	✓	✓	×	✓	×	×	✓

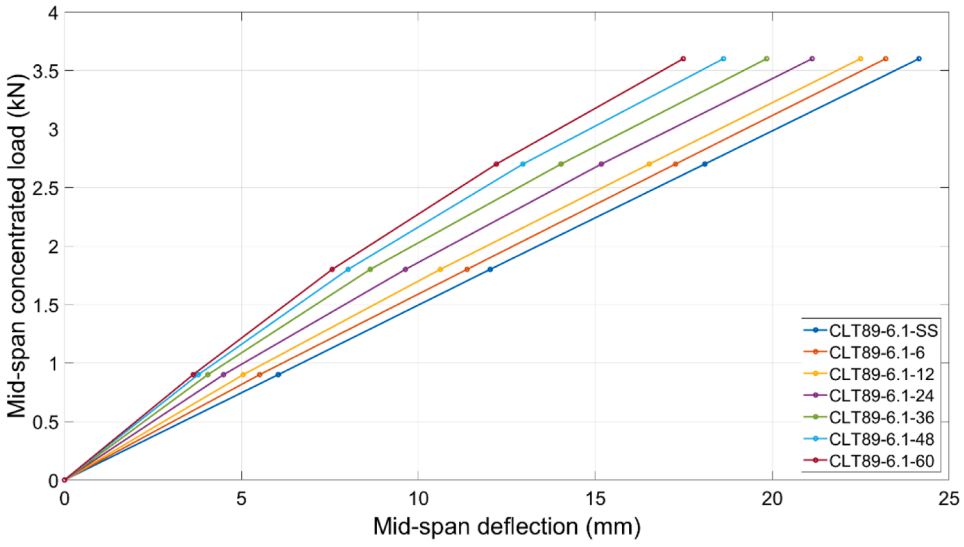

(a) Load-deflection curves

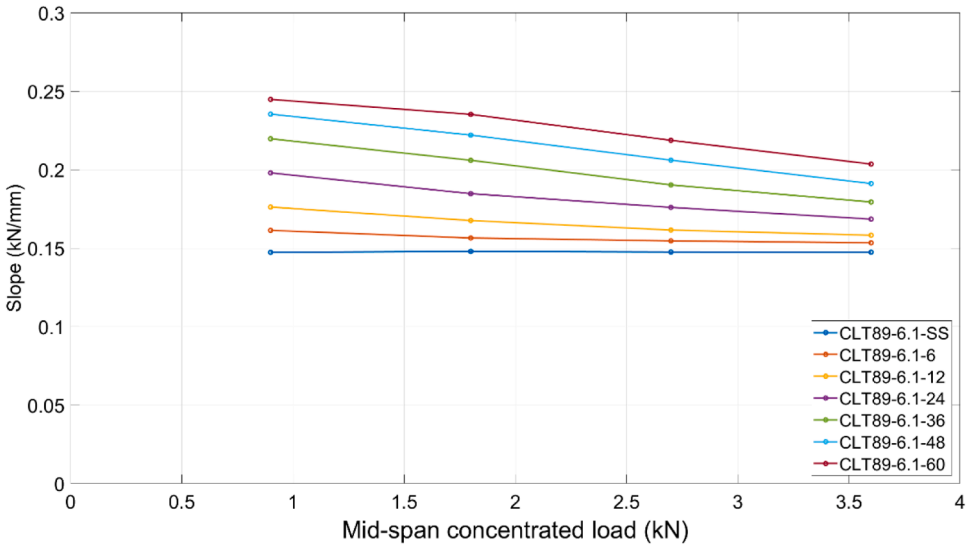

(b) Slope

Fig. 8. Load-deflection curves and their slopes for the CLT89–6.1 assembly.

deflection) with different sensitivities [26,27]. In this study, both static and dynamic techniques were applied to determine the rotational stiffness at end supports. It is not difficult to learn that the end-support rotational stiffness obtained using static deflection may not be identical with that derived from natural frequency.

Furthermore, as discussed in preceding section, end fixity factors exhibit non-linear behaviours and gradually decreases with an increase in concentrated loads. Therefore, if different levels of concentrated loads are used to evaluate the floor performance, the end fixity factors will inevitably change due to the rotational stiffness degradation. Hence, in this study, the end fixity factors were separately determined for static deflection and fundamental natural frequency and denoted as r_d and r_f, as shown in Eqs. (6) and (7). The values of r_d and r_f are presented in Table A to Table E in Appendix A.

A scatter plot as shown in Fig. 10 presents the comparisons between r_d and r_f for all end support configurations tested for CLT89, CLT105, CLT175 and CLT244 assemblies. It can be found that the points are widely spread around the line of identity ($r_f = r_d$), and only a few of them cluster closely the line. This indicates a significant difference between r_d and r_f, with the absolute values of the difference mostly larger than 20%, as seen from the dotted lines. Further observation suggests that more than half of the points lie to the left of the line of equality, which means that for the same configuration, r_f is mostly larger than r_d.

5. Governing factors of end support restraints

To achieve a clearer understanding of the governing relations and reduce complexity, it is necessary to identify the critical factors that quantify the influence of end support restraints, with a focus on capturing the most important features. The impact of end support conditions is affected by numerous factors such as the level of top loads over supports, installation of STS, provision of SAB, and other fastening techniques. It is noticeable that the restrained effect through top loads plays a major role in end support restraints, and screws and brackets

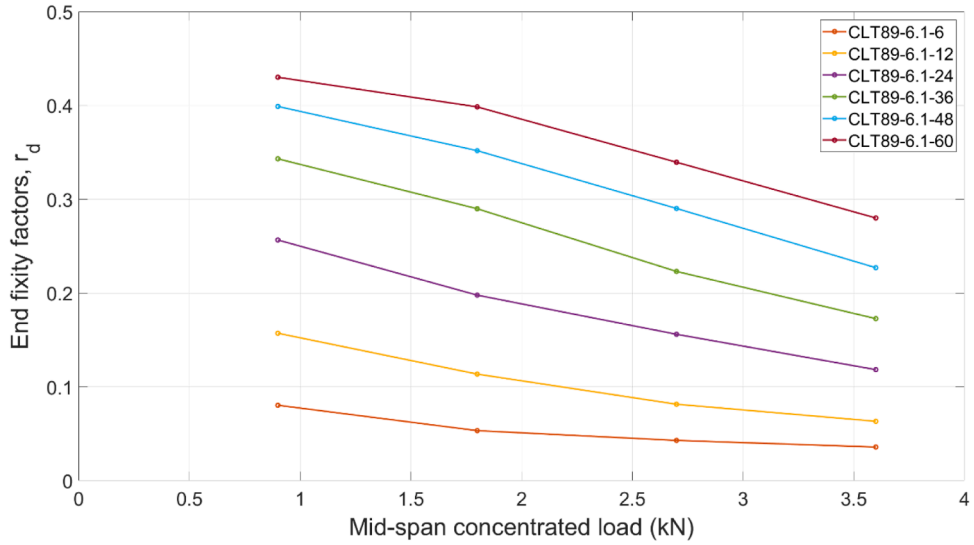

Fig. 9. End fixity factors, r_d, for CLT89–6.1 assembly under different concentrated loads.

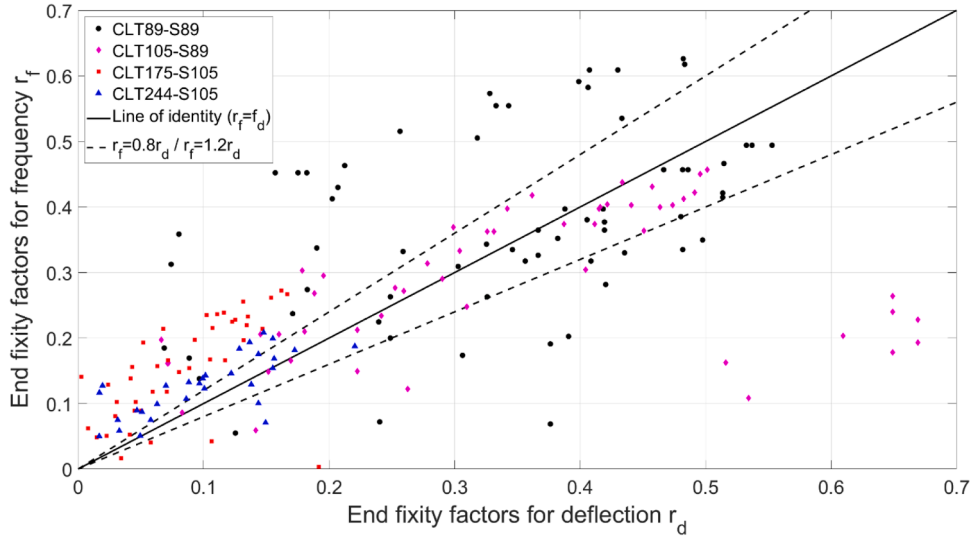

Fig. 10. Comparison of r_d and r_f (the line of identity indicates complete agreement between r_d and r_f; the dotted line of $r_f = 0.8r_d$ is below the line of identity and the dotted line of $r_f = 1.2r_d$ lies to the top of the line of identity).

would be relatively minor factors. Therefore, the effect of top load was first examined in the following sections. It should be noted that since short-span floors are unlikely to be vulnerable to human-induced vibrations, specimens with a 2.4 m span (i.e., CLT89–2.4, CLT105–2.4 and CLT175–2.4) were not considered herein.

5.1. *Effect of end-support load levels*

In this study, top loads were varied between 0 kN/m (simple support) and 60 kN/m, and its effect was characterized by end-fixity factors. The relationship between end fixity factors and top load levels is shown in Fig. 11. As expected, the end fixity factors increase with higher top load levels, and the relationship between them is nonlinear. The increasing rate of the end-fixity factor declines with an increase in top loads, especially for CLT89 and CLT105 assemblies for r_f in Fig. 11b. This suggests that small load increases produce appreciable increases in the end-fixity factor when the top load level is low, say less than 10 kN/m. On the contrary, significant load changes result in small shifts in the end-fixity factor with high levels of top loads, higher than 10 kN/m. More importantly, for the same load level, the end-fixity factor decreases with any significant increase in the thickness of CLT panels (i.e., CLT89 and CLT105 vs CLT175 and CLT244), leading to widely spread values.

5.2. *Effect of floor thickness and span*

A notable trend, as depicted in Fig. 11, is the substantially lower end fixity factors observed for CLT175 and CLT244 assemblies (red curves) compared to CLT89 and CLT105 assemblies (black curves). This is primarily attributed to the increased weight or flexural stiffness of the thicker floor slabs, which reduces the restraining effect of the top loads.

Moreover, it can be observed from Fig. 11 that, although the end support restraint caused by a top load is a localized effect, it is also influenced by the span. Similar observations were reported in [11], where it was found that the rotational stiffness determined by Hernandez and Chui [15] was affected by the span. This influence probably stems from the indirect measurement of end support restraints in the tests. With varying floor span, the effect of external loads on end supports is different. As shown in Fig. 12, it can be observed that for the same top loads at the support and external forces on the floor, the longer the span is, the greater moment can be created by the external load at the

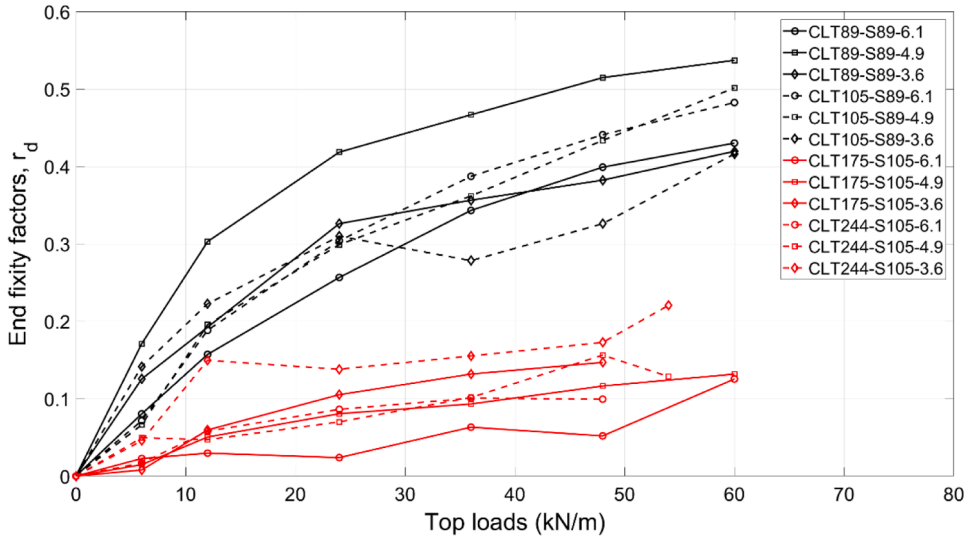

(a) End fixity factors for deflection, r_d

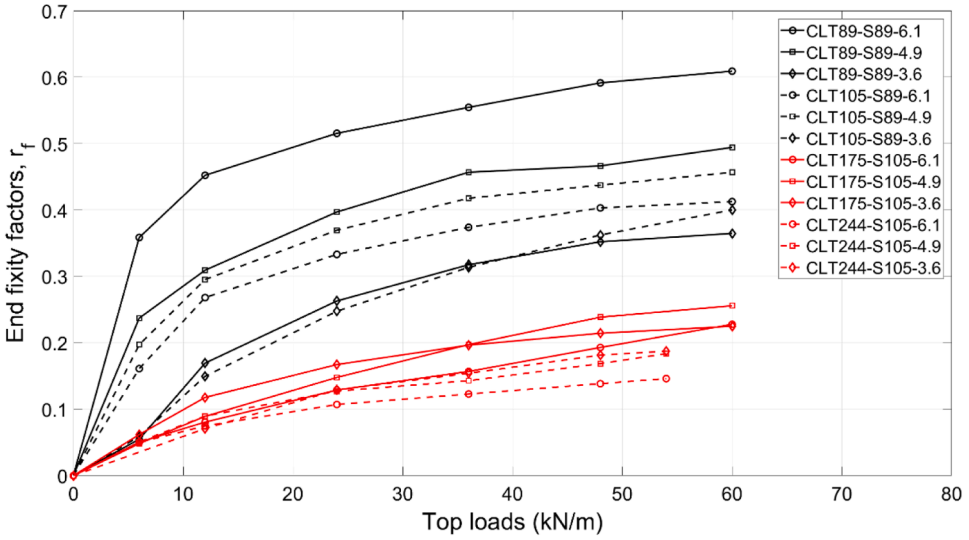

(b) End fixity factors for frequency, r_f

Fig. 11. End fixity factors of CLT floor-to-wall assemblies with different top loads: (a) r_d and (b) r_f.

support pivot point *O*, resulting in a greater restraining demand. Due to the nonlinear behaviour of the floor-to-wall connections as discussed in Section 4.1, the stiffness of the end support restraint varies with different floor spans.

However, despite the additional tests conducted in the current stage, no certain relations can be established between end support restraints and floor spans. Further investigations are needed, and it is also important to consider the panel thickness, especially when external loading is small (e.g., 1 kN at the mid-span for vibration serviceability design).

5.3. Dominant role of top loads

The clamping effect of top loads on the floor is dominant when compared to STS and SAB. However, it remains unclear whether the domination of top loads diminishes at small load levels. To examine the dominance of different top load levels, tests were conducted for top loads combining with SABs. Three load levels were studied: 12 kN/m, 36 kN/m and 60 kN/m. The restrained effects of these loads were tested first, and then SABs were installed. Fig. 13 compares the end-fixity factors of top loads with SAB (3SAB or 5SAB) to those without SABs. Table 4 presents mean values and coefficient of variation (CoV) of end-fixity factor ratios, which is defined as the ratio of loading support configurations with SAB (e.g., CLT89–6.1–12 +3SAB) over the corresponding one without SABs (e.g., CLT89–6.1–12). The increase in end-fixity factors for deflections, r_d, due to installing SABs was found to be small and negligible for higher top loads (e.g., 36 kN/m and 60 kN/m in Table 4). Similarly, the increase in end-fixity factors related to frequency, r_f, due to SABs is consistently negligible, regardless of the top load level, as shown in Fig. 13b and Table 4.

Furthermore, while direct fastening using STS serves as the primary connection between floor slabs and wall panels beneath, the installation of SABs connects the wall above to the floor slab, and it is expected to exert a smaller impact on end restraints. The test results in Table A show that the end-fixity factor values remain consistent for CLT89–6.1–60 + 5STS, with or without 5SAB. Hence, the effect of SABs

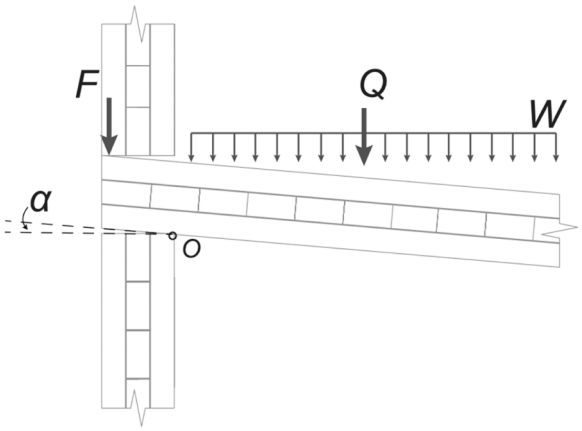

Fig. 12. Schematic diagram of a mass timber floor-to-wall connection (*F* is the top load, *W* is self-weight, *Q* is external loads and *O* is the pivot point).

is minimal and can be neglected.

On the other hand, in relation to STS, the domination of end support loads is highly dependent on the top load level. Table 5 presents end fixity factor ratios of top loads with STS to those without STS (i.e., 12/36/60 +5STS and 12/36/60), along with their mean values and variance. Despite the large data variance (e.g., CoV=52%), a clear trend can be observed that the ratios are significantly higher for lower end-support loads (i.e., 12 kN/m) and close to 1 for the top load of 60 kN/m. This suggests that the effect of STS is significant for small top loads but minimal for high top loads, which can be attributed to the nonlinear

Table 4
End fixity factor ratio of top load with SAB to that without SAB.

Top loads (kN/m)	r_d ratios		r_f ratios	
	Mean	CoV (%)	Mean	CoV (%)
12	1.15	12	0.99	14
36	1.09	15	1.02	4
60	1.01	11	1.00	5

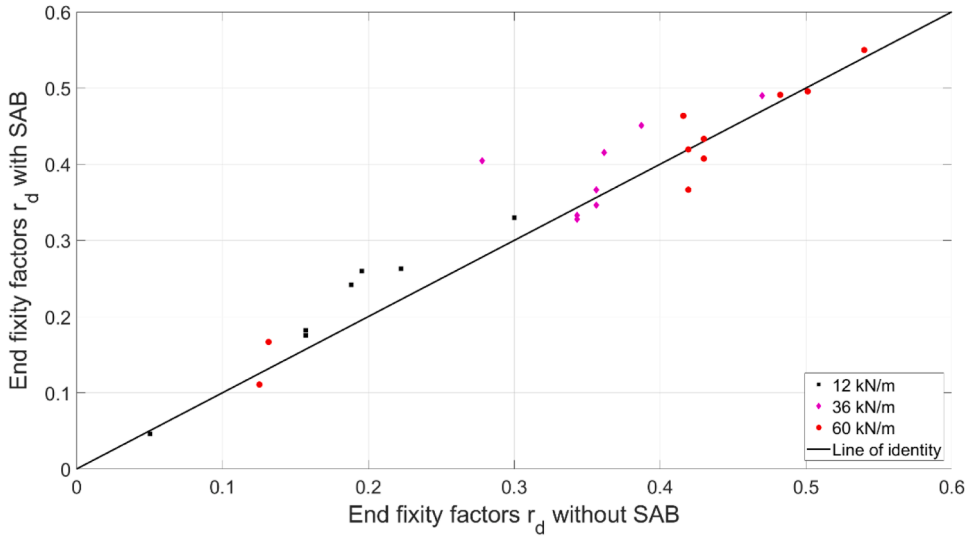

(a) End fixity factors for deflections

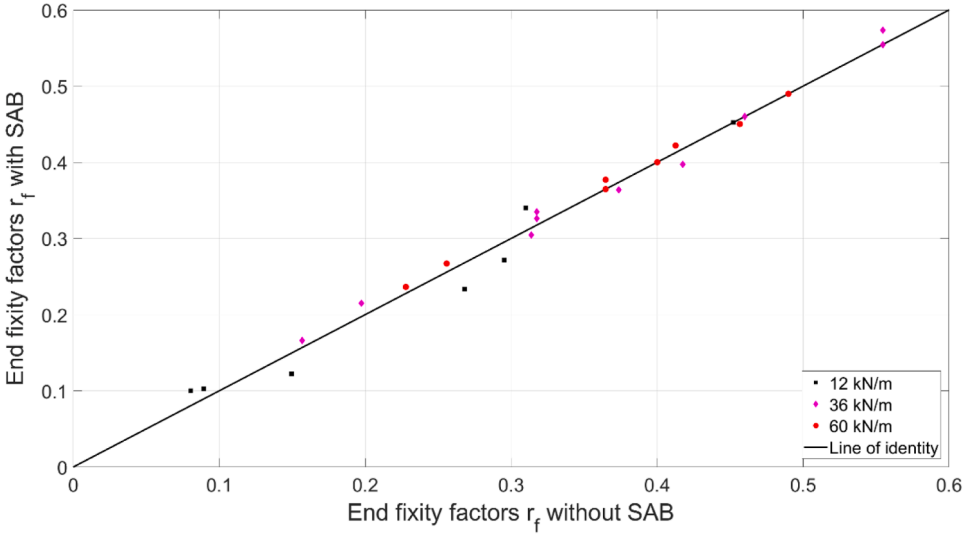

(b) End fixity factors for frequency

Fig. 13. Comparisons between end-fixity factor with top load and SAB and that with top load without SAB.

Table 5
End fixity factors ratios of top loads with STS to those without STS (e.g., ratio of CLT89–6.1-S89 +12 +5STS to CLT89–6.1-S89 +12).

Assemblies	r_d ratios			r_f ratios		
	12 + 5STS to 12	36 + 5STS to 36	60 + 5STS to 60	12 + 5STS to 12	36 + 5STS to 36	60 + 5STS to 60
CLT89-S89–6.1	2.02	1.18	1.12	1.12	1.05	1.01
CLT89-S89–4.9	1.28	1.03	0.99	1.28	1.00	1.00
CLT89-S89–3.6	2.81	1.15	1.15	1.55	1.00	1.06
CLT105-S89–6.1	1.54	1.06	0.98	1.08	1.00	0.98
CLT105-S89–4.9	0.91	0.95	0.91	1.03	0.95	0.94
CLT105-S89–3.6	1.14	1.19	1.01	1.85	1.16	1.01
CLT175-S105–6.1	3.95	2.13	1.23	2.06	1.40	1.15
CLT175-S105–4.9	1.76	1.45	1.23	1.73	1.18	1.07
CLT175-S105–3.6	/	/	/	1.32	1.09	1.05
CLT244-S105–6.1	1.09	0.96	1.61†	1.32	1.06	1.00†
CLT244-S105–4.9	1.88	1.35	1.15†	1.48	1.35	1.13†
CLT244-S105–3.6	0.96	0.93	0.70†	1.42	1.14	1.06†
Mean	1.76	1.22	1.10	1.44	1.12	1.04
CoV(%)	52	28	21	22	13	6

Notes: / - not listed due to large errors as shown in Table D
† - results of 54 kN/m

impact of the top loads discussed earlier. Consequently, when the top load is low, installation of STS generates considerable restraints, but these restrained effects decrease as the top load increases. In summary, although the end support load dominates the restrained effect, the effect of STS cannot be ignored, especially for small top loads.

5.4. Effects of self-tapping screws (STS)

The previous section discussed the restrained effect of STS combined with top loads, which is a common configuration in construction practice. However, for research purposes, it is also useful to examine the effect of STS alone. Table 6 presents the end-fixity factors of support configurations with different numbers of STS (i.e., 3STS and 5STS). It can be found that end-fixity factors increase with increase in number of screws, particularly for the fundamental natural frequency. Only two exceptions were noted for r_d, which may be due to the viscoelastic behaviour of timber panels. In addition, the influence of the STS length was examined for CLT105 assemblies, as shown in Table 7. Longer screws resulted in larger end-fixity factors, but the improvement was much smaller when adding the end support load. Two exceptions were highlighted in red.

5.5. Effects of support wall thickness

Both end support walls made from 105-3s and 175–5s CLT panels (referred to as S105 and S175) were provided for CLT175 and CLT244 assemblies to investigate the influence of support wall thickness. Their respective end-fixity factors are listed in Table D and Table E in Appendix A. The results indicate that the end-fixity factors of the assemblies with S175 are significantly greater than those with S105.

Fig. 14 presents a comparison between the end-fixity factor ratios of S175 and S105 assemblies. It can be observed that points spread to the left of the line of identity with a few exceptions on the right side, suggesting that the thicker support walls (i.e., S175) resulted in larger end support restraints. This effect can be attributed to several factors. One notable factor could be the reduction in the clear span between the inner faces of the supports, which resulted in smaller mid-span deflection and higher natural frequencies, despite using the same end support load or connector for assemblies with different support wall thickness. It should be noted that end restraint coefficients C_d and C_f were directly determined based on the ratios of measured deflection and frequency of a restrained beam to those of a simply supported beam, as described in Section 4.2, without taking into account the possible reduction in the clear span due to end support restraints.

In this study, the floor-to-wall connection is modelled as a lengthless rotational spring, and the beam span, thus far, has been defined as the distance from center to center of the wall supports for both simply supported and restrained conditions, as shown in Fig. 3. It is essential to note that when the floor is restrained by the upper and lower support walls through connectors or top loads, the floor section on the wall supports should be considered as part of the support restraint, rather than the floor slab itself. As such, coefficients C_d and C_f obtained from measured deflection and frequency included the effect of the reduction in the clear span, which may be the primary reason for the coefficient difference and the resulting variations in end fixity factors r_d and r_f. Considering the span reduction due to the support thickness, the clear span was then used in Eqs. (1) and (2). They can be rewritten as

$$d_{1kN} = C_d \frac{PL_c^3}{48EI} \tag{8}$$

$$f_1 = C_f \frac{\pi}{2L_c^2}\sqrt{\frac{EI}{\rho A}} \tag{9}$$

where L_c is the clear span. In this manner, modified values of C_d and C_f can be obtained.

Fig. 15 and Fig. 16 illustrate the restraint coefficient ratios of S175 assemblies to S105 ones. There ratios are observed to spread out on both sides of 1 (noting that larger end support restraints result in smaller C_d or larger C_f). The figures also show the ratios of modified values for S175 assemblies to those with S105. It can be found that the ratios of modified

Table 6
End-fixity factor results of support configurations with different numbers of self-tapping screws (ratio values less than 1 were marked as red.).

Assemblies	r_d		Ratio†	r_f		Ratio†
	3STS	5STS		3STS	5STS	
CLT89–6.1-S89	0.21	0.21	1.00	0.43	0.46	1.08
CLT89–4.9-S89	0.18	0.26	1.42	0.27	0.33	1.21
CLT89–3.6-S89	0.10	0.07	0.71	0.14	0.18	1.34
CLT105–6.1-S89	0.15	0.18	1.19	0.15	0.21	1.42
CLT105–4.9-S89	0.07	0.15	2.02	0.16	0.21	1.27
CLT105–3.6-S89	0.17	0.22	1.31	0.17	0.21	1.28
CLT175–6.1-S105	0.06	0.04	0.72	0.04	0.14	3.42
CLT175–4.9-S105	0.04	/	/	0.09	0.10	1.15
CLT175–3.6-S105	0.07	/	/	0.12	0.14	1.20
CLT244–6.1-S105	0.03	0.03	1.00	0.06	0.07	1.28
CLT244–4.9-S105	0.02	0.02	1.00	0.12	0.13	1.09
CLT244–3.6-S105	0.05	/	/	0.09	0.13	1.44
Mean:			1.17			1.43
CoV(%):			34			45

Notes: † - ratio of end fixity factors of 5STS to those of 3STS
/ - not used due to large errors as shown in Table D and Table E

Table 7
End fixity factors of CLT105 with different screw lengths (PTS8160–160 mm and PTS8240–240 mm as shown in Table 1).

Support configurations		r_d		Difference (%)	r_f		Difference (%)
		PTS8160	PTS8240		PTS8160	PTS8240	
STS	6.1–3STS	0.12	0.15	26	0.12	0.15	24
	4.9–3STS	0.07	0.07	3	0.08	0.16	103
	3.6–3STS	0.10	0.17	69	0.25	0.17	-33
	6.1–5STS	0.15	0.18	20	0.19	0.21	11
Top loads	6.1–12 + 5STS	0.31	0.29	-6	0.26	0.29	13
+	6.1–36 + 5STS	0.40	0.41	2	0.33	0.37	12
STS	6.1–60 + 5STS	0.46	0.47	2	0.40	0.40	0

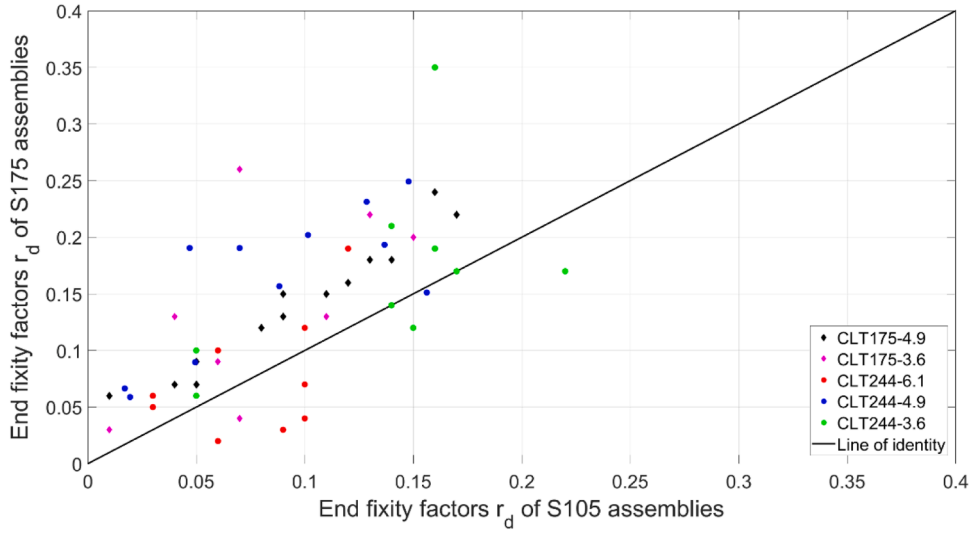

(c) End fixity factors for deflections

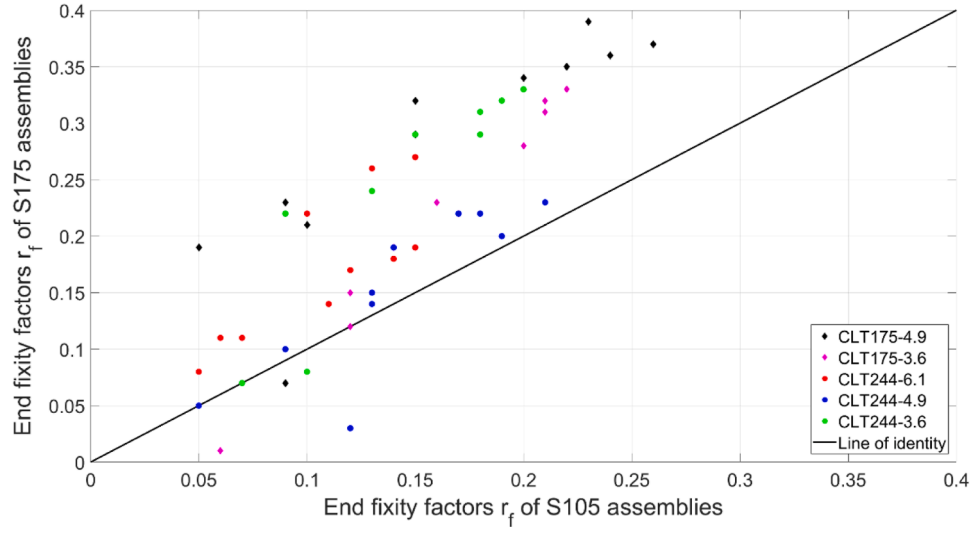

(d) End fixity factors for frequency

Fig. 14. Comparisons between end-fixity factor of S175 assemblies and that of S105 assemblies.

C_d and C_f are generally much closer to 1, except for CLT 244–6.1 and CLT 244–3.6 in Fig. 15 and CLT 244–4.9 in Fig. 16, which requires further investigations.

Overall, it can be concluded that support wall thickness significantly influences end support restraints, with thicker support walls generally resulting in larger end support restraints. Using the clear span in calculation appears to be an effective way to account for the wall thickness, but further investigation is needed.

6. Conclusions

This paper presents a comprehensive experimental study aimed at quantifying end support restraints and their influence on the vibration serviceability of mass timber floors. Four CLT panels of varying

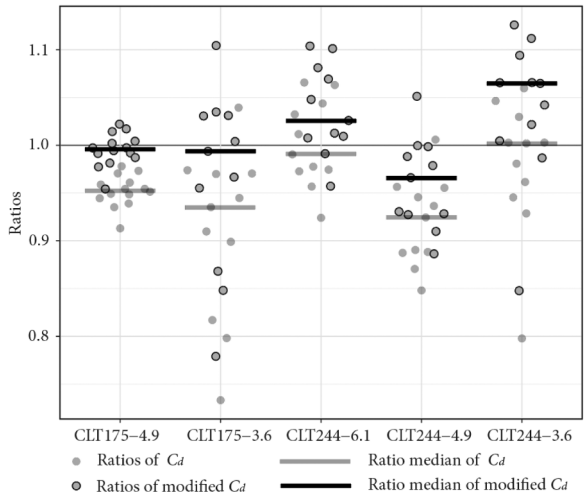

Fig. 15. C_d ratios of assemblies with S175 wall to those with S105.

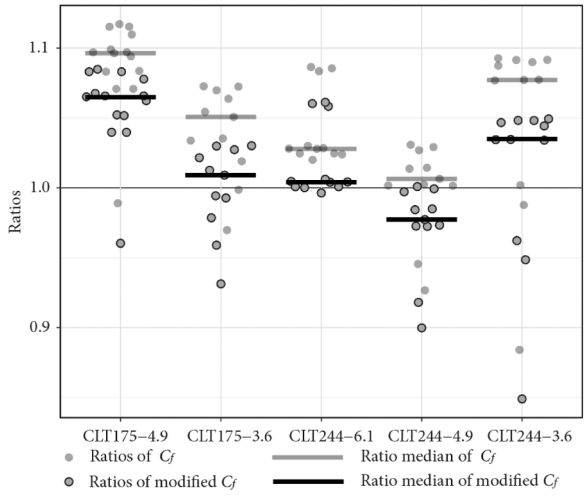

Fig. 16. C_f ratios of assemblies with S175 wall to those with S105.

thicknesses were tested at different spans, with an examination of over 100 end support configurations. The influences of top loads, self-tapping screws and steel angle brackets were investigated to gain a more profound understanding of the underlying relationships. The critical factors for quantifying the influence of end support restraints were identified and captured, which will be used to derive empirical formulas in future research based on these test results.

The test results show that CLT floor-to-wall connections exhibit inherent non-linear behaviour over a whole range of loading levels at mid-span, similar to other semi-rigid connections. The rotational stiffness gradually decreases with the increase of concentrated load applied at mid-span, and this non-linear characteristic is more pronounced with higher top loads on the supports. The value of rotational stiffness, represented by end-fixity factors, should be determined with specified loading level on the floors. For vibration serviceability design, the mid-span loads commonly set at 1 kN. It is also observed that end-fixity factors determined from fundamental natural frequency are generally larger than those determined from mid-span deflection. This suggests that end support restraints should differ for static deflection and natural frequency calculations.

Top loads have a predominant impact on end support restraints, and a larger top load results in a significant increase in the support restraint. However, this relationship is non-linear. When the end support loading level is low (less than 10 kN/m), a small load increase produces an appreciable increase in the restraint factor. On the contrary, at high levels of top load, a substantial load change may result in a small change in the restraint factor.

The influence of self-tapping screws is significant but diminishes with an increase in the top load level. A greater number of self-tapping screws improve the end support restraint, and the screw length also has a positive influence on the support restraint. A longer screw leads to a larger end fixity factor, although this improvement is more modest when a top load is also present. At last, the effect of steel bracket is minimal and can be neglected, no matter how large the top loads are.

Other factors such as support wall thickness, floor slab thickness, and span also have some influence on end support restraints. Notably, a wider support results in a greater restraint, mainly due to the reduction in the clear span. To account for the support thickness, it is recommended to use the clear span for determining the deflection and frequency for restrained boundary conditions for mass timber floors, rather than the center-to-center length used for the simply supported condition.

The end fixity factor decreases significantly with a substantial increase in the thickness of floor slabs, resulting in widely varying values for the same load level. Since the end support restraints were indirectly measured, the floor span affects these restraint values. However, no general trend can be observed in the current investigation.

The ultimate goal of the present study is to develop empirical design formulas that consider the partially restrained effect on mass timber floor-to-wall connections. After capturing the most-important features through tests, the remaining effort will be dedicated to deriving formulas for the vibration serviceability design of mass timber floors to account for the improvement in performance resulting from an increase in end fixity. This work on the derivation of formulas will be presented in a forthcoming publication.

CRediT authorship contribution statement

Zhang Sigong: Conceptualization, Data curation, Formal analysis, Investigation, Methodology, Writing – original draft, Writing – review & editing. **Chui Ying Hei:** Conceptualization, Funding acquisition, Project administration, Resources, Supervision, Writing – review & editing.

Declaration of Competing Interest

The authors declare that they have no known competing financial interests or personal relationships that could have appeared to influence the work reported in this paper.

Data availability

Data will be made available on request.

Acknowledgements

This research was supported through funding from the Natural Sciences and Engineering Research Council to NSERC Industrial Research Chair in Engineered Wood and Building Systems at the University of Alberta. A special gratitude towards Nordic Structures and Rotho Blaas for providing the test materials. The assistance provided by Ning Kang, Jialin Li and Linlin Ma towards the test program is gratefully acknowledged. The first author gratefully acknowledges the support from Canada Emergency Response Benefit (CERB) during the COVID-19 pandemic.

Statement

During the preparation of this work the author(s) used ChatGBT in order to proofreading. After using this tool/service, the author(s) reviewed and edited the content as needed and take(s) full responsibility

for the content of the publication.

Appendix A – Results of end fixity factors

Based on Eqs. (6) and (7), end-fixity factors were determined for 1 kN mid-span deflection and fundamental natural frequency, and the results are presented in Table A to Table E for all test assemblies and their associated end support configurations. Values with significant errors are marked in red color and were not used in analysis.

Table A End fixity factors of CLT89-S89 assemblies.

End support configurations	CLT89-6.1		CLT89-4.9		CLT89-3.6		CLT89-2.4	
	r_d	r_f	r_d	r_f	r_d	r_f	r_d	r_f
SS	0	0	0	0	0	0	0	0
6	0.08	0.36	0.17	0.24	0.13	0.05	0.28	**-0.07**
12	0.16	0.45	0.30	0.31	**0.09**	0.17	0.31	0.17
24	0.26	0.52	0.42	0.40	0.33	0.26	0.38	0.19
36	0.34	0.55	0.47	0.46	0.36	0.32	0.42	0.28
48	0.40	0.59	0.51	0.47	0.38	0.35	0.48	0.34
60	0.43	0.61	0.54	0.49	0.42	0.36	0.41	0.38
60 + 3SAB	0.43	0.54	0.55	0.49	0.42	0.38	0.51	0.42
36 + 3SAB	0.33	0.57	0.49	0.46	0.35	0.34	0.50	0.35
12 + 3SAB	0.18	0.45	0.33	0.34	0.24	0.22	0.39	0.20
12 + 5SAB	0.18	0.45	/	/	0.25	0.20	0.38	0.07
36 + 5SAB	0.33	0.55	/	/	0.37	0.33	0.44	0.33
60 + 5SAB	0.41	0.61	/	/	0.37	0.36	0.51	0.41
3STS	0.21	0.43	0.18	0.27	0.10	0.14	0.07	0.31
5STS	0.21	0.46	0.26	0.33	0.07	0.18	**-0.07**	0.35
12 + 5STS	0.32	0.51	0.39	0.40	0.25	0.26	0.24	**0.07**
36 + 5STS	0.41	0.58	0.48	0.46	0.41	0.32	0.19	0.34
60 + 5STS	0.48	0.62	0.53	0.49	0.48	0.39	0.20	0.41
60 + 5STS+ 5SAB	0.48	0.63	/	/	/	/	/	/

Notes: r_d – end fixity factors for mid-span 1 kN deflection
r_f – end fixity factors for fundamental natural frequency
/ – not tested

Table B End fixity factors of CLT105-S89 assemblies.

End support configurations	CLT105-6.1		CLT105-4.9		CLT105-3.6		CLT105-2.4	
	r_d	r_f	r_d	r_f	r_d	r_f	r_d	r_f
SS	0	0	0	0	0	0	0	0
6	0.07	0.16	0.07	0.20	0.14	0.06	0.13	**-0.43**
12	0.19	0.27	0.20	0.30	0.22	0.15	**0.08**	**-0.19**
24	0.30	0.33	0.30	0.37	0.31	0.25	0.53	0.11
36	0.39	0.37	0.36	0.42	0.28	0.31	0.52	0.16
48	0.44	0.40	0.43	0.44	0.33	0.36	0.61	0.20
60	0.48	0.41	0.50	0.46	0.42	0.40	0.67	0.23
60 + 3SAB	0.49	0.42	0.50	0.45	0.46	0.40	0.65	0.26
36 + 3SAB	0.45	0.36	0.42	0.40	0.40	0.30	0.67	0.19
12 + 3SAB	0.24	0.23	0.26	0.27	0.26	0.12	0.32	**-0.04**
3STS	0.15	0.15	0.07	0.16	0.17	0.17	0.16	0.21
5STS	0.18	0.21	0.15	0.21	0.22	0.21	0.08	0.09
12 + 5STS	0.29	0.29	0.18	0.30	0.25	0.28	0.21	**-0.10**
36 + 5STS	0.41	0.37	0.34	0.40	0.33	0.36	0.65	0.18
60 + 5STS	0.47	0.40	0.46	0.43	0.42	0.40	0.65	0.24

Notes: r_d – end fixity factors for mid-span 1 kN deflection
r_f – end fixity factors for fundamental natural frequency

Table C End fixity factors of CLT105-S89 assemblies with PTS8160.

End support configurations	CLT105-6.1		CLT105-4.9		CLT105-3.6		CLT105-2.4	
	r_d	r_f	r_d	r_f	r_d	r_f	r_d	r_f
3STS	0.12	0.12	0.07	0.08	0.10	0.25	0.07	/
5STS	0.15	0.19	/	/	/	/	/	/
12 + 5STS	0.31	0.26	/	/	/	/	/	/
36 + 5STS	0.40	0.33	/	/	/	/	/	/
60 + 5STS	0.46	0.40	/	/	/	/	/	/

Notes: r_d – end fixity factors for mid-span 1 kN deflection
r_f – end fixity factors for fundamental natural frequency
/ – not tested

Table D End fixity factors of CLT175 assemblies.

End support configurations	CLT175-6.1		CLT175-4.9		CLT175-3.6		CLT175-2.4	
	r_d	r_f	r_d	r_f	r_d	r_f	r_d	r_f
CLT175-S105								
SS	0	0	0	0	0	0	0	0
6	0.02	0.05	0.01	0.05	0.01	0.06	0.03	**-0.70**
12	0.03	0.08	0.05	0.09	0.06	0.12	0.06	**-0.37**
24	0.02	0.13	0.08	0.15	0.11	0.17	0.19	**-0.14**
36	0.06	0.16	0.09	0.20	0.13	0.20	0.22	**-0.02**
48	0.05	0.19	0.12	0.24	0.15	0.21	0.29	**0**
54	/	/	/	/	/	/	0.19	**0**
60	0.13	0.23	0.13	0.26	**0.12**	0.22	/	/
60 + 3SAB	0.11	0.24	0.17	0.27	/	/	/	/
36 + 3SAB	0.07	0.17	0.11	0.22	/	/	/	/
12 + 3SAB	**0**	0.10	0.05	0.10	/	/	/	/
3STS	0.06	0.04	0.04	0.09	0.07	0.12	0.03	0.02
5STS	0.04	0.14	**0.03**	0.10	**0**	0.14	0.04	0.05
12 + 5STS	0.12	0.17	0.09	0.15	0.04	0.16	0.16	**-0.34**
36 + 5STS	0.13	0.22	0.14	0.23	0.07	0.21	0.18	**-0.01**
54 + 5STS	/	/	/	/	0.10	0.24	0.11	0.04
60 + 5STS	0.15	0.26	0.16	0.27	/	/	/	/
CLT175-S175								
SS	/	/	0	0	0	0	/	/
6	/	/	0.06	0.19	0.03	0.01	/	/
12	/	/	0.07	0.23	0.09	0.12	/	/
24	/	/	0.12	0.29	0.13	0.22	/	/
36	/	/	0.15	0.34	0.22	0.28	/	/
48	/	/	0.16	0.36	0.20	0.32	/	/
60	/	/	0.18	0.37	0.38	0.33	/	/
60 + 3SAB	/	/	0.22	0.42	/	/	/	/
36 + 3SAB	/	/	0.15	0.35	/	/	/	/
12 + 3SAB	/	/	0.09	0.21	/	/	/	/
3STS	/	/	0.07	0.07	0.04	0.15	/	/
5STS	/	/	0.06	0.21	0.05	0.19	/	/
12 + 5STS	/	/	0.13	0.32	0.13	0.23	/	/
36 + 5STS	/	/	0.18	0.39	0.26	0.31	/	/
60 + 5STS	/	/	0.24	0.43	0.28	0.34	/	/

Notes: d_{1kN} – mid-span 1 kN deflection
f_1 – fundamental natural frequency
/ – not tested

Table E End fixity factors of CLT244 assemblies.

End support configurations	CLT244-6.1		CLT244-4.9		CLT244-3.6	
	r_d	r_f	r_d	r_f	r_d	r_f
CLT244-S105						
SS	0	0	0	0	0	0
6	0.02	0.05	0.05	0.05	0.05	**-0.03**
12	0.06	0.07	0.05	0.09	0.15	0.07
24	0.09	0.11	0.07	0.13	0.14	0.13
36	0.10	0.12	0.10	0.14	0.16	0.15
48	0.10	0.14	0.16	0.17	0.17	0.18
54	**0.08**	0.15	0.13	0.18	0.22	0.19
3STS	0.03	0.06	0.02	0.12	0.05	0.09
5STS	0.03	0.07	0.02	0.13	**0.03**	0.13
12 + 5STS	0.06	0.10	0.09	0.13	0.14	**0.10**
36 + 5STS	0.10	0.13	0.14	0.19	0.14	0.18
54 + 5STS	0.12	0.15	0.15	0.21	0.16	0.20
CLT244-S175						
SS	0	0	0	0	0	0
6	0.01	0.08	0.09	0.05	0.06	**-0.24**
12	0.02	0.11	0.19	0.10	0.12	0.07
24	0.03	0.14	0.19	0.15	0.14	0.24
36	0.04	0.17	0.20	0.19	0.19	0.29
48	0.07	0.18	0.15	0.22	0.17	0.31
54	0.08	0.19	0.23	0.22	0.17	0.32
3STS	0.06	0.11	0.07	0.03	0.10	0.22
5STS	0.05	0.11	0.06	0.00	**-0.02**	0.24
12 + 5STS	0.10	0.22	0.16	0.14	0.14	0.08
36 + 5STS	0.12	0.26	0.19	0.20	0.21	0.29
60 + 5STS	0.19	0.27	0.25	0.23	0.35	0.33

Notes: d_{1kN} – mid-span 1 kN deflection
f_1 – fundamental natural frequency
/ – not tested

References

[1] Harte AM. Mass timber–the emergence of a modern construction material. J Struct Integr Maint 2017;2(3):121–32.
[2] Karacabeyli E, Gagnon S. CLT handbook, 2019 Edition, Vol. 1. . Pointe-Claire, QC: FPinnovations,; 2019.
[3] Chiniforush AA, Alamdari MM, Dackermann U, Valipour HR, Akbarnezhad A. Vibration behaviour of steel-timber composite floors, part (1): Experimental & numerical investigation. J Constr Steel Res 2019;161:244–57.
[4] Hu LJ, Chui YH, Onysko DM. Vibration serviceability of timber floors in residential construction. Prog Struct Eng Mater 2001;3(3):228–37.
[5] Weckendorf J, Toratti T, Smith I, Tannert T. Vibration serviceability performance of timber floors. Eur J Wood Wood Prod 2016;74(3):353–67.
[6] Hu LJ, Chui YH, Hamm P, Toratti T, Orskaug T. Development of ISO baseline vibration design method for timber floors. Aug 20-23 Proc 2018 World Conf Timber Eng (WCTE2018), Seoul, Korea 2018. Aug 20-23.
[7] Negreira J, Trollé A, Jarnerö K, Sjökvist LG, Bard D. Psycho-vibratory evaluation of timber floors–Towards the determination of design indicators of vibration acceptability and vibration annoyance. J Sound Vib 2015;340:383–408.
[8] Homb A, Kolstad ST. Evaluation of floor vibration properties using measurements and calculations. Eng Struct 2018;175:168–76.
[9] Hu LJ, Gagnon S. Controlling cross-laminated timber (CLT) floor vibrations: fundamentals and method. Proc 2012 World Conf Timber Eng (WCTE) Auckl, NZ 2012:269–75.
[10] CSA O86–19. Engineering Design in Wood, Canadian Standard Association. Mississauga, Ontario, Canada, 2019.
[11] Zhang S, Zhou J, Niederwestberg J, Chui YH. Effect of end support restraints on vibration performance of cross laminated timber floors: An analytical approach. Eng Struct 2019;189:186–94.
[12] Brandner R, Flatscher G, Ringhofer A, Schickhofer G, Thiel A. Cross laminated timber (CLT): overview and development. Eur J Wood Wood Prod 2016;74(3):331–51.
[13] Weckendorf J, Smith I. Dynamic characteristics of shallow floors with cross-laminated-timber spines. Auckland, New Zealand: The proceedings of 2012 world conference on timber engineering (WCTE2012),; 2012.
[14] Hernández SAM, Chui YH. Vibrational performance of cross laminated timber floors. Auckland, New Zealand: The proceedings of 2012 world conference on timber engineering (WCTE2012),; 2012.
[15] Hernández SAM, Chui YH. Effect of end support conditions on the vibrational performance of cross-laminated timber floors. Quebec City, Canada: The proceedings of 2014 world conference on timber engineering (WCTE2014),; 2014.
[16] Zimmer S, Augustin M. Vibrational behaviour of cross laminated timber floors in residential buildings. Vienna, Austria: The proceedings of 2016 world conference on timber engineering (WCTE2016),; 2016.
[17] Chúláin CU, Harte AM. Experimental investigation of the serviceability behaviour of a cross laminated timber floor. Dublin: Civil engineering research in Ireland CERI-ITRN 2018. University College,; 2018.
[18] Chúláin CU, Sikora K, Harte AM. Influence of connection systems on serviceability response of CLT timber flooring. Vienna, Austria: The proceedings of 2016 world conference on timber engineering (WCTE),; 2016.
[19] Ussher E, Arjomandi K, Weckendorf J, Smith I. Predicting effects of design variables on modal responses of CLT floors. Structures 2017;11:40–8.
[20] Thiel A, Zimmer S, Augustin M, Schickhofer G. CLT and floor vibration: A comparison of design methods. Vancouver, Canada: Proceedings of international council for research and innovation in building and construction working commission W18-Timber Structures (CIB-W18),; 2013. p. 381–92.
[21] Malo KA, Köhler J. Vibrations of timber floor beams with end restraints. Structures and Architecture: Concepts, Applications and Challenges–Proceedings of the 2nd International Conference on Structures and Architecture, ICSA. London: CRC Press,; 2013.
[22] APA (The Engineered Wood Association). Standard for performance-rated cross-laminated timber. Tacoma, WA: ANSI/APA PRG-320,; 2018.
[23] Jones SW, Kirby PA, Nethercort DA. The analysis of frames with semi-rigid connections—a state-of-the-art report. J Constr Steel Res 1983;3(2):2–13.
[24] Wang L, Guo N, Yang Z. Boundary condition identification of tapered beam with flexible supports using static flexibility measurements. Mech Syst Signal Process 2016;75:138–54.
[25] Mertlich TB, Halling MW, Barr PJ. Dynamic and static behavior of a curved-girder bridge with varying boundary conditions. J Perform Constr Facil 2007;21(3):185–92.
[26] Waters TP, Brennan MJ, Sasananan S. Identifying the foundation stiffness of a partially embedded post from vibration measurements. J Sound Vib 2004;274(1–2):137–61.
[27] Liu W, Yang Z, Wang L, Guo N. Boundary condition modelling and identification for cantilever-like structures using natural frequencies. Chin J Aeronaut 2019;32(6):1451–64.